AIP | Applied Physics Letters

Plasmonic fiber-optic vector magnetometer

Zhaochuan Zhang, Tuan Guo, Xuejun Zhang, Jian Xu, Wenping Xie, Ming Nie, Qiang Wu, Bai-Ou Guan, and Jacques Albert

Citation: Applied Physics Letters **108**, 101105 (2016); doi: 10.1063/1.4943623
View online: http://dx.doi.org/10.1063/1.4943623
View Table of Contents: http://scitation.aip.org/content/aip/journal/apl/108/10?ver=pdfcov
Published by the AIP Publishing

Plasmonic fiber-optic vector magnetometer

Zhaochuan Zhang,[1] Tuan Guo,[1,a)] Xuejun Zhang,[1] Jian Xu,[1] Wenping Xie,[2] Ming Nie,[2] Qiang Wu,[3] Bai-Ou Guan,[1] and Jacques Albert[4]
[1]*Institute of Photonics Technology, Jinan University, Guangzhou 510632, China*
[2]*Electric Power Research Institute of Guangdong Power Grid Company Limited, Guangzhou 510080, China*
[3]*Department of Physics and Electrical Engineering, Northumbria University, Newcastle Upon Tyne NE1 8ST, United Kingdom*
[4]*Department of Electronics, Carleton University, 1125 Colonel By Drive, Ottawa K1S 5B6, Canada*

(Received 24 December 2015; accepted 23 February 2016; published online 10 March 2016)

A compact fiber-optic vector magnetometer based on directional scattering between polarized plasmon waves and ferro-magnetic nanoparticles is demonstrated. The sensor configuration reported in this work uses a short section of tilted fiber Bragg grating (TFBG) coated with a nanometer scale gold film and packaged with a magnetic fluid (Fe_3O_4) inside a capillary. The transmission spectrum of the sensor provides a fine comb of narrowband resonances that overlap with a broader absorption of the surface plasmon resonance (SPR). The wavelength of the SPR attenuation in transmission shows high sensitivity to slight perturbations by magnetic fields, due to the strong directional scattering between the SPR attenuated cladding modes and the magnetic fluid near the fiber surface. Both the orientation (2 nm/deg) and the intensity (1.8 nm/mT) of magnetic fields can be determined unambiguously from the TFBG spectrum. Temperature cross sensitivity can be referenced out by monitoring the wavelength of the core mode resonance simultaneously. © *2016 AIP Publishing LLC*.
[http://dx.doi.org/10.1063/1.4943623]

A magnetic field is a fundamental physical quantity used in a diverse range of applications and its measurement has generated consistent interest over the years. Such measurements often involve magnetic fluids, a kind of stable colloid that typically consists of magnetic nanoparticles (i.e., Fe_3O_4) dressed with surfactant and highly dispersed in a liquid carrier.[1] Magnetic field sensors based on the magnetic fluid materials have been widely studied due to the fact that convenient magneto-optical effects can be utilized, such as a tunable refractive index (RI),[2] tunable thermal properties,[3] and tunable transmission loss.[4] In particular, magnetic fluids are easy to integrate with optical fibers and high sensitivity, miniature, non-electrical fiber magnetic field sensors have been proposed recently. Taking advantage of the tunable RI of magnetic fluids, magnetic sensors based on the magnetic fluid infiltration into the micro-holes of photonic crystal fibers (PCFs) have been well studied.[5–9] Meanwhile, various kinds of fiber-grating based magnetic sensors have been proposed, such as using long-period fiber gratings (LPG)[10–12] or etched fiber Bragg gratings.[13] Moreover, interference-based fiber-optic magnetic sensing structures such as tapered fibers and Fabry-Perot interferometers have also been proposed.[14–24] However, all of the above mentioned structures suffer from a certain amount of complexity that makes them less than ideal in real applications, for instance the need for fluid infiltration into micro-holes of PCF or the additional packaging required to protect weakened tapered or etched fibers. Furthermore, all the previous devices have some temperature cross-sensitivity that needs to be compensated for. The tilted fiber Bragg grating (TFBG) is a more recent kind of fiber-optic sensor that possesses all the advantages of the well-established Bragg grating technology in addition to having inherent multi-parameter sensing capability and negligible temperature cross-sensitivity. This is because the TFBGs resonantly excite a large number of cladding modes in the fiber with a phase and amplitude that can be measured with high precision from the transmission spectrum of the TFBG. These features result in an extreme sensitivity to materials external to the fiber (high RI sensitivity) without an extra manufacturing process to the fiber to be etched or tapered (thus maintaining the robustness and reproducibility of the fabricated sensors).[25–27]

In this work, a single plasmonic TFBG surrounded by the magnetic fluid is used to measure both the intensity and orientation of imposed magnetic fields. The transduction mechanism is based on the wavelength signature of a surface plasmon resonance (SPR) that is observed in the transmission spectra of TFBGs with the nanoscale metal coatings, and it shows a much improved sensitivity than the previously reported intensity-based detection techniques, even those using the TFBG magneto-optic sensors.[28–31] More importantly, the breaking of the fiber cylindrical symmetry arising from the grating inscription of the TFBG leads to a strong in-fiber polarization of the cladding modes and provides the possibility of measuring the direction of the magnetic field, much like a compass.[32] These improvements in the TFBG sensing performance come from the fact that with the presence of nano-scale metal coatings (i.e., gold or silver) some modes in the TFBG spectral response transfer significantly (tens of %, i.e., one order of magnitude more than "normal" evanescent waves) to a surface plasmon wave of the metal-external medium interface.[33–36] The key point of the present work is that the external magnetic fields re-arrange the distribution and density of the disordered Fe_3O_4 nanoparticles around the fiber surface into the ordered chains oriented in a

[a)]Author to whom correspondence should be addressed. Electronic mail: tuanguo@jnu.edu.cn

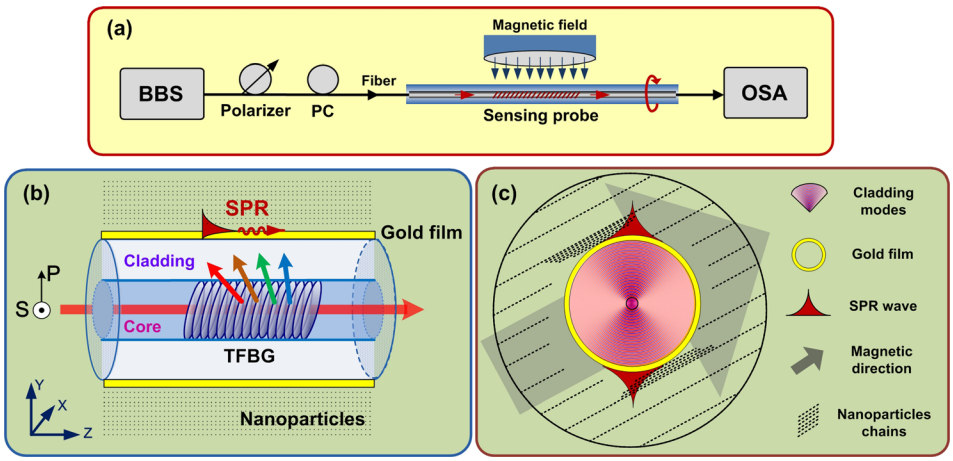

FIG. 1. (a) Schematic diagram of magnetic sensing system; (b) polarimetric TFBG with linearly polarized light emitting for SPR excitations; (c) cross section of TFBG and ferro-nanoparticles sealed in a capillary tube under an external magnetic field.

direction parallel to the applied magnetic field. The localized accumulation of the particles causes a strong optical scattering of the polarized surface plasmons and consequentially of the TFBG spectrum. Red or blue shifts of the SPR feature in the fiber transmission spectra show unequivocally the exact orientation difference between the grating tilt plane and the applied magnetic field. As a consequence, both the orientation and the intensity of the magnetic field can be determined via simple monitoring of the wavelength shift of the SPR in the TFBG spectrum during a full rotation of the device in the field to be measured. The detailed transduction principle and interrogation scheme are presented in the following.

The experimental setup of the magnetic field measurement based on a 15° TFBG is illustrated in Fig. 1(a). Light from a broadband source (BBS) is launched in the sensing TFBG and its transmission spectrum is monitored by an optical spectrum analyzer (OSA) with a resolution of 0.01 nm. A linear polarizer and polarization controller (PC) are placed upstream of the TFBG to control and orient the state of polarization of the light launched into the fiber grating. The TFBG is packaged in a capillary tube which is filled with the magnetic fluid and sealed with glue on both sides to prevent leakage. A straight, homogeneous magnetic field with an adjustable intensity and orientation is applied perpendicularly to the fiber axis. A Gauss meter with a resolution of 0.1 mT is used to measure the magnetic field intensity along the field axis. The TFBG packaged in the capillary tube is kept fixed during the experiment, immune from any unwanted fiber bending or strain. Since all the resonances of a TFBG have the same temperature dependence (≈10 pm/°C), spectral shifts due to the environmental temperature changes can be eliminated by referencing all wavelengths to the core mode reflection wavelength.

The TFBGs were inscribed by a KrF excimer laser using the phase-mask method over a hydrogen-loading standard single mode fiber. As shown in Fig. 1(b), due to the introduction of the tilt angle between the UV laser beam and the fiber axis, the TFBG provides an effective way of coupling light from the incident core mode to cladding modes. Furthermore, due to the breakup of the circular symmetry of the fiber, the polarization state of the incident core mode controls the orientation and polarization of the excited cladding modes at the cladding boundary. P-polarized light predominantly excites the cladding modes with radial electrical fields, while S-polarized light excites cladding modes for which the electrical field is tangential to the cladding boundary. Therefore, the P-polarized light can transfer energy to the surface plasmon wave on the metal surface, but S-polarized light cannot. The magnetic fluid used in this experiment (EMG705, Ferrotec, Japan, with saturation magnetization of 22 mT and effective RI of 1.385) is a water-based ferrofluid with nanoparticles (Fe_3O_4) about 10 nm in diameter. Fig. 1(c) shows the cross section of gold-coated TFBG surrounded by the ferro-nanoparticles. Due to the inherent coupling properties of the TFBG, the cladding modes have most of their power distributed in two lobes oriented along the vertical direction in the figure, and consequently the same holds for the plasmon waves excited at the resonant wavelengths, as shown in Fig. 1(c). When an external magnetic field is applied, the nanoparticles agglomerate and form chains along the direction of the magnetic field, along the dashed dotted lines shown in Fig. 1(c).

Fig. 2 shows that the transmission of a gold-coated TFBG under S-polarized light presents no SPR attenuation of the cladding mode resonances (because tangentially polarized light cannot penetrate through the metal layer). For this polarization, there is no sensitivity to the surrounding RI changes, including those due to re-arrangements of the nanoparticles. But for the P-polarized light the transmission shows a very clear SPR attenuation at wavelengths near

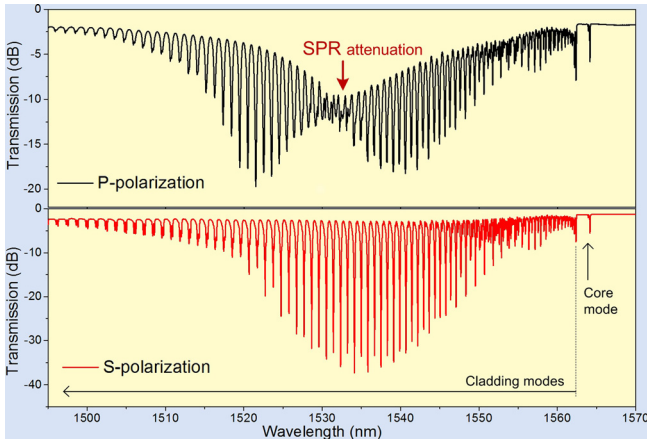

FIG. 2. Transmission spectra of TFBG coated with 50 nm of gold and immersed in magnetic fluid, for P-polarized incident light (top) and S-polarized incident light (bottom). The SPR location corresponds to the spectral notch near 1530 nm in the upper graph.

1530 nm when the fiber is immersed in magnetic fluid with RI of 1.385 (the top black spectrum). It should be noted that the TFBG provides a fine comb of narrowband resonances that overlap with the broader absorption of the SPR and thus provides a unique tool to measure small shifts of SPR with high accuracy (here the cladding resonance located at 1531 nm can be used to pinpoint the SPR wavelength for sensing). At the same time, due to the scattering effect between the cladding modes (including the surface plasmon wave) and the Fe_3O_4 nanoparticles, the P-polarized transmission presents an overall higher insertion loss than the S-polarization one, but this effect does not prevent accurate measurements of the resonance positions.

As shown in Fig. 3(a) (and the corresponding image on the right of the spectrum), when there is no magnetic field the distribution of magnetic particles is relatively uniform and the SPR position can be established. When an external magnetic field is applied, the magnetic particles agglomerate on the sides of the fiber that are parallel with the applied magnetic field, and disappear from the parts of the fiber circumference that are perpendicular to it. Together with the results shown in Figs. 3(b) and 3(c) (Multimedia view), it appears that gathering nanoparticles over the SPR fiber surface (magnetic field parallel to x axis) will increase the average refractive index over this area (due to RI of magnetic fluid is larger than that of water), resulting in a longer wavelength shift of SPR resonance, while moving the nanoparticles away from the plasmon field (magnetic field parallel to y axis) decreased the average refractive index near the SPR fiber surface and shifts the SPR to shorter wavelengths. The microscopic images of bubbles in the magnetic fluid under various magnetic fields and direction, shown on the right side of Fig. 3, support this interpretation of the behavior of the particles around the fiber. To obtain those images, the magnetic fluid is placed between a glass slide and a cover glass, and an air bubble is created intentionally to simulate the distribution of Fe_3O_4 nanoparticles around the fiber surface under the external magnetic fields. As shown in microscope images, the magnetic particles will form chain-like clusters along with the direction of magnetic field. Moreover, because of the fluid discontinuity (bubble or fiber surface), the particles are attracted to the surface, and in greater numbers with increasing magnetic field. This last finding is confirmed by the results of Fig. 4.

Fig. 4(a) shows the wavelength shift of the SPR with increasing magnetic field intensity for three different magnetic field orientations. In the experiment, the field orientation (as determined by the arms of the electromagnet used to generate the field) remains unchanged, and the field intensities increased from 0 to 18 mT. As shown in Fig. 4(a), when the magnetic field is oriented vertically (i.e., in the tilt direction of the grating), the SPR resonance shifts to shorter wavelengths by 4 nm. On the other hand, when the magnetic field is oriented horizontally (perpendicular to the tilt direction), the SPR resonance shifts to longer wavelengths by 22 nm, providing the maximum intensity sensitivity of 1.8 nm/mT. When the field is oriented at 45° or 135° relative to the tilt plane, there is no change in the SPR position.

Fig. 4(b) (Multimedia view) shows the sensor response directional sensitivity (from 0° to 360°), for two values of magnetic field intensity. Noting that the wavelength shifts occurring between 45° and 135° and between 225° and 315° are negative, the combined results of Fig. 4 show that this fiber optic magnetometer can be used to detect the orientation of the magnetic field direction (with a maximum orientation sensitivity of 2 nm/deg and an uncertainty of 180°, i.e., it cannot discriminate the sign of the magnetic field intensity) and its magnitude, at least in the range from 2 to 18 mT. It must also be pointed out that full orientation capability cannot be performed in a static measurement because there are many points in Fig. 4(b) that have equal wavelength shifts. Therefore, a rotation of the sensor to locate the direction of the maximum (or minimum) wavelength shift is required to locate the magnetic field direction. Once this is

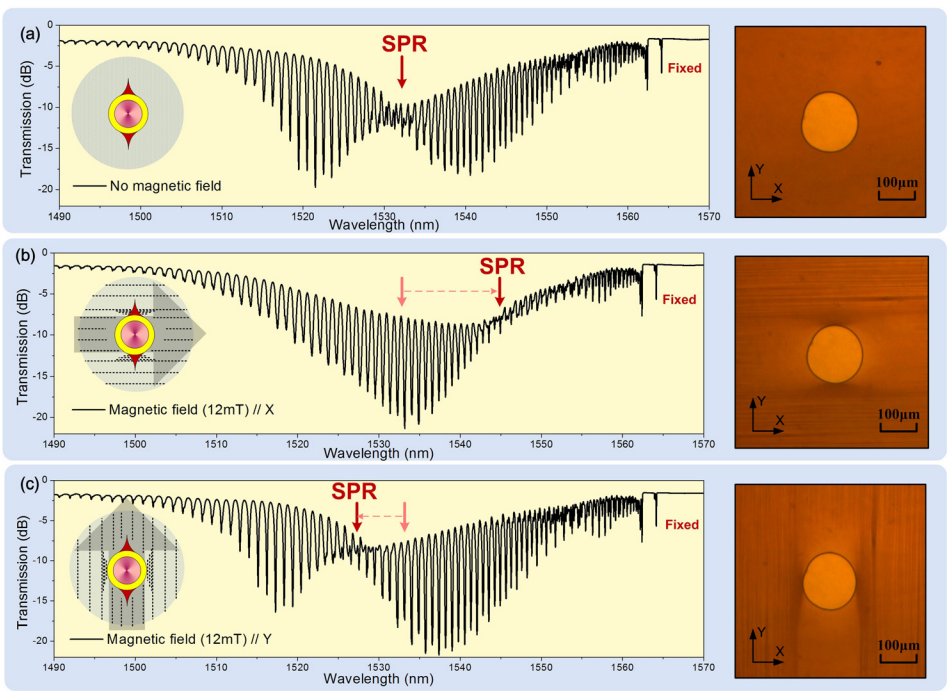

FIG. 3. Left: Plasmonic TFBG spectral responses: (a) without magnetic field, (b) with magnetic field along the horizontal (X) direction, (c) with magnetic field in the vertical (Y) direction. Right: microscope image of the magnetic fluid clusters formed around an air bubble (with diameter close to a standard SMF). (Multimedia view) [URL: http://dx.doi.org/10.1063/1.4943623.1]

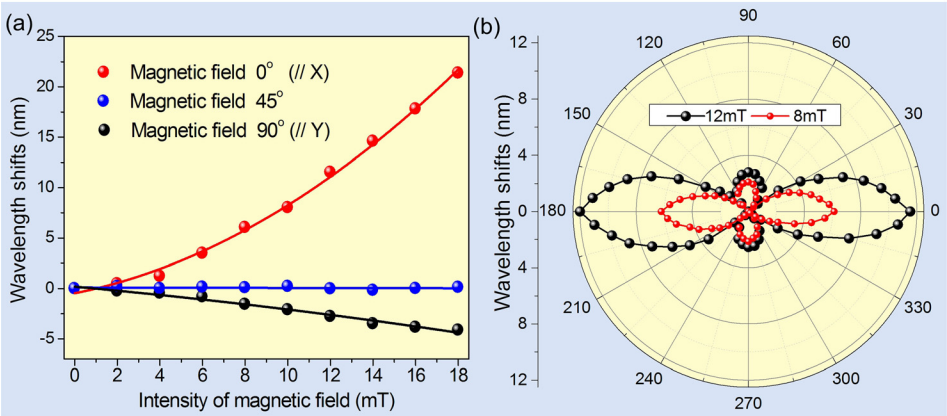

FIG. 4. (a) Wavelength shift of the TFBG-SPR to magnetic field intensity for three different orientations; (b) absolute value of the wavelength shift to magnetic field orientation (with TFBG tilt plane at 90°), for two values of magnetic field intensity. (Multimedia view) [URL: http://dx.doi.org/10.1063/1.4943623.2]

done, there is a one-to-one relationship between the magnitude of the wavelength shift and of the magnetic field intensity. The measurement can also self-calibrate since the ratio of the maximum positive wavelength shift to the maximum negative shift (occurring at 90° from the maximum) is immune to source or system power level fluctuations. Finally, it should be noted that by tracking the amplitude change of a single cladding mode (modulated by the SPR), the sensor can further improve its sensitivity for measuring a quite small magnetic field changes.

The feasibility of a plasmonic fiber-optic vector magnetometer using only a short section of gold-coated TFBG packaged in a capillary tube filled with magnetic fluid (Fe_3O_4) is experimentally demonstrated. The results observed are explained by the interaction between the evanescent field of a surface plasmon wave excited in a nanoscale gold coating of the fiber and magnetic nanoparticles suspended in a fluid that surrounds the fiber. The device is made from a standard optical fiber, tilted FBGs, and a conventional metallization process, while interrogation is carried out using the standard telecom based light sources and detectors. This device further benefits from the usual fiber optic sensor properties of compact size, high sensitivity, and remote interrogation, while adding TFBG specific benefits such as temperature and power self-calibration.

This work was funded by the National Natural Science Foundation of China (No. 61235005), the Applied Science and Technology Research Foundation of Guangdong (No. 2015B010127014), the Natural Science Foundation of Guangdong (No. 2014A030313387), the Youth Science and Technology Innovation Talents of Guangdong (No. 2014TQ01X539), the Fundamental Research Funds for the Central Universities of China (No. 21615446). Q. Wu acknowledges the support of the Open Fund of IPOC (BUPT). J. Albert acknowledges the support of the Natural Sciences and Engineering Research Council of Canada (No. RGPIN 2014-05612) and the Canada Research Chairs Program (No. 950-217783).

[1]B. Hoffmann and W. Köhler, J. Magn. Magn. Mater. **262**, 289 (2003).
[2]S. Y. Yang, J. J. Chieh, and H. E. Horng, Appl. Phys. Lett. **84**, 5204 (2004).
[3]J. Philip, P. D. Shima, and B. Raj, Appl. Phys. Lett. **92**, 043108 (2008).
[4]S. Y. Yang, Y. P. Chiu, B. Y. Jeang, and H. E. Horng, Appl. Phys. Lett. **79**, 2372 (2001).
[5]A. Candiani, A. Argyros, S. G. Leon-Saval, R. Lwin, S. Selleri, and S. Pissadakis, Appl. Phys. Lett. **104**, 111106 (2014).
[6]P. Zu, C. C. Chan, T. Gong, Y. Jin, W. Wong, and X. Dong, Appl. Phys. Lett. **101**, 241118 (2012).
[7]H. V. Thakur, S. M. Nalawade, S. Gupta, R. Kitture, and S. N. Kale, Appl. Phys. Lett. **99**, 161101 (2011).
[8]A. Candiani, M. Konstantaki, W. Margulis, and S. Pissadakis, Opt. Lett. **37**, 4467 (2012).
[9]P. Zu, C. C. Chan, W. S. Lew, L. Hu, Y. Jin, H. F. Liew, L. H. Chen, W. C. Wong, and X. Dong, IEEE Photonics J. **4**, 491 (2012).
[10]T. Liu, X. Chen, Z. Di, J. Zhang, X. Li, and J. Chen, Appl. Phys. Lett. **91**, 121116 (2007).
[11]L. Gao, T. Zhu, M. Deng, K. S. Chiang, X. Sun, X. Dong, and Y. Hou, IEEE Photonics J. **4**, 2095 (2012).
[12]Y. Miao, K. Zhang, B. Liu, W. Lin, H. Zhang, Y. Lu, and J. Yao, IEEE Photonics Technol. Lett. **25**, 306 (2013).
[13]J. Dai, M. Yang, X. Li, H. Liu, and X. Tong, Opt. Fiber Technol. **17**, 210 (2011).
[14]M. Deng, D. Liu, and D. Li, Sens. Actuators, A **211**, 55 (2014).
[15]S. Dong, S. Pu, and H. Wang, Opt. Express **22**, 19108 (2014).
[16]Y. Zhao, R. Lv, D. Wang, and Q. Wang, IEEE Trans. Instrum. Meas. **63**, 2210 (2014).
[17]D. Homa and G. Pickrell, Sensors **14**, 3891 (2014).
[18]R. Q. Lv, Y. Zhao, D. Wang, and Q. Wang, IEEE Photonics Technol. Lett. **26**, 217 (2014).
[19]Y. Zhao, R. Q. Lv, Y. Ying, and Q. Wang, Opt. Laser Technol. **44**, 899 (2012).
[20]L. Azam, H. Latifi, and O. Frazao, IEEE Photonics Technol. Lett. **26**, 1904 (2014).
[21]W. Lin, Y. Miao., H. Zhang, B. Liu, Y. Liu, and B. Song, Appl. Phys. Lett. **103**, 151101 (2013).
[22]J. J. Chieh, S. Y. Yang, H. E. Horng, C. Y. Hong, and H. C. Yang, Appl. Phys. Lett. **90**, 133505 (2007).
[23]Y. Miao, J. Wu, W. Lin, K. Zhang, Y. Yuan, B. Song, H. Zhang, B. Liu, and J. Yao, Opt. Express. **21**, 29914 (2013).
[24]S. Pu and S. Dong, IEEE Photonics J. **6**, 1 (2014).
[25]J. Albert, L. Y. Shao, and C. Caucheteur, Laser Photonics Rev. **7**, 83 (2013).
[26]T. Guo, F. Liu, B. O. Guan, and J. Albert, Opt. Laser Technol. **78**, 19 (2016).
[27]J. Albert, S. Lepinay, C. Caucheteur, and M. C. DeRosa, Methods **63**, 239 (2013).
[28]W. Lin, Y. Miao, H. Zhang, B. Liu, Y. Liu, B. Song, and J. Wu, J. Lightwave Technol. **31**, 2599 (2013).
[29]J. Zheng, X. Dong, P. Zu, L. Y. Shao, C. C. Chan, Y. Cui, and P. P. Shum, Opt. Express **21**, 17863 (2013).
[30]D. Yang, L. Du, Z. Xu, Y. Jiang, J. Xu, M. Wang, Y. Bai, and H. Wang, Appl. Phys. Lett. **104**, 061903 (2014).
[31]J. Zheng, X. Dong, P. Zu, J. Ji, H. Su, and P. P. Shum, Appl. Phys. Lett. **103**, 183511 (2013).
[32]Y. Li, M. Froggatt, and T. Erdogan, J. Lightwave Technol. **19**, 1580 (2001).
[33]C. Caucheteur, V. Voisin, and J. Albert, Opt. Express **21**, 3055 (2013).
[34]C. Caucheteur, C. Chen, V. Voisin, P. Berini, and J. Albert, Appl. Phys. Lett. **99**, 041118 (2011).
[35]C. Caucheteur, T. Guo, and J. Albert, Anal. Bioanal. Chem. **407**, 3883 (2015).
[36]Y. Y. Shevchenko and J. Albert, Opt. Lett. **32**, 211 (2007).